Examination of aerosol effects on the development of supercell storm using the WRF Double-Moment (WDM) microphysics schemes

Kyo-Sun Sunny Lim[1,] Song-You Hong[1], Seong-Soo Yum[1], and Jimy Dudhia[2]

[1]Department of Atmospheric Sciences, Yonsei University, Seoul, Korea

[2]Mesoscale and Microscale Meteorology Division/NCAR, Boulder, Colorado, USA

1. Introduction

Aerosol effects on large-scale stratiform clouds studied via several climate models (Menon 2004; Lohmann and Feichter 2005; Takemura et al. 2005) suggest that the suppression of precipitation with increased aerosols can alter the radiative fluxes due to changes in cloud lifetime or liquid water path. It is not certain whether the suppression of precipitation applies for deep convective cloud with increasing aerosol concentration. It is worth noting that most previous studies of aerosol-cloud interaction were primarily concentrated on warm and stratiform clouds. Generally speaking, despite the critical role of deep convective clouds in general circulation as well as the Earth-atmospheric radiative and hydrological budget, studies of aerosol-cloud interaction in this type of clouds are still in demand.

Recently, aerosol effects on deep convective clouds have been evaluated through several observational and modeling works (Khain et al. 2005; Wang 2005; Feingold 2006). However, the formation and development of precipitation in convective clouds to increased aerosols do not follow the same process as in stratiform or warm clouds. Aerosol effects on cloud microphysics and precipitation could be non-monotonic under the different meteorological and aerosol conditions, because of the complicated coupling between the cloud microphysics and storm dynamics (Seifert and Beheng 2006; Fan et al. 2007; van den Heever and Cotton 2007; Lee et al. 2008).

The purpose of this study is to investigate the aerosol effects on the development of supercell storm, focusing on the storm morphology and precipitation. Supercell thunderstorm, which is characterized by a deep, persistent, rotating updraft, is in fact the most prolific procedures of denser ice particles such as graupel and hail. Thus, the Weather Research and Forecasting (WRF) Double-Moment 6-class (WDM6) Microphysics scheme (Lim and Hong 2009), which includes the graupel substance, will be used. Even though several previous studies stressed the importance of the microphysical drop size distribution (or size itself) and evaporative cooling rates on tornadogenesis (van den Heever and Cotton 2004; Snook and Xue 2008), Few studies, which concerned aerosol-related microphysical effects on the evolution of supercell storms, have been reported (Lerach et al. 2008).

This paper is organized as follows. Section 2 outlines the numerical experiments conducted in this study, and their results are discussed in Section 3. Concluding remarks appear in the final section.

2. Numerical experimental setup

The model used in this study is the Advanced Research WRF version 3.1 (ARW; Skamarock et al. 2008). The 3D idealized supercell thunderstorm, which is a preset option for the WRF model, was designed to investigate aerosol effects by changing the initial value of the CCN number concentration. The grid in both directions comprised 81 points with a 2 km grid spacing. The number of vertical layers was 40. The model was integrated for 2 hours with a time step of 12 seconds. The environmental wind makes a quarter circle when plotted on a hodograph, and is commonly referred to as quarter circle shear. For the vertical profiles of potential temperature and the water vapor mixing ratio, we adopted same soundings as Weisman and Klemp (1986). A symmetric temperature perturbation of 2 K and 10 km radius triggers deep convection in a potentially unstable environment.

In addition to the WDM6 microphysics scheme, mixed phase WRF Double-Moment 5-class Microphysics (WDM5) scheme was also tested. The differences between the WDM6 and WDM5 scheme is the existence of graupel and graupel-related microphysics processes. Simulations were initiated with the nine different initial CCN number concentrations from 100 cm^{-3} to 10000 cm^{-3}. Impact of the initial aerosol concentrations on the development of supercell storm is evaluated by varying the number and mass of aerosols, as is reflected in the changes in the number concentrations of CCN. Three experiments such as

Corresponding Author: Kyo-Sun Sunny Lim
E-mail: klim@yonsei.ac.kr

WDM6_M, WDM6_C, and WDM6_EC, will be mainly discussed. The WDM6_M run employs the initial number concentration of CCN as 100 cm^{-3}, the WDM6_C as 2000 cm^{-3}, and the WDM6_EC as 10000 cm^{-3}. The name of CCN experiments with the WDM5 scheme is given in a same manner.

An additional sensitivity experiment, the WDM6_VG experiment with a pre-described CCN number concentration as 100 cm^{-3}, was performed to explore the effect of faster sedimentation velocity of graupel than that of snow. The values of the empirical constants for the terminal velocities of graupel and its density were replaced with the ones of snow.

3. Results

a. CCN effects

Figures 1a and b show the storm structure defined with low level rain water fields, maximum vertical velocities, and storm-relative surface wind vectors in the WDM6_M and WDM6_EC runs at 2 hour. The WDM6_M run shows the similar storm structure, compared with previous study. The initial storm evolves into a right-moving, quasi-steady supercell with two diverging echo masses. The left storm moves to the northeastern direction and right one to the eastern direction. Updraft develops along the right (left)-flank storm's right (left)-flank in response to the gust front convergence. Meanwhile, the intensity of the left storm is stronger compared with the simulation presented by Weisman and Kemp (1986). The WDM6_EC run, which is initiated with the 100 times lager CCN number concentration than the WDM6_M run, shows different distribution of low-level rain water fields with a ambiguous splitting of the two convective cores and sporadic rain water fields near the eyewall region from the WDM6_M run (Fig. 1d). A relatively strong downdraft was produced at approximately 60 km along the Y-direction due to strong evaporative cooling rates of rain drops in the WDM6_M run, providing a favorable environment for tornadogenesis, where the low-level mesocyclone and near-surface vorticity induced by the strong downdraft remained vertically-stacked (Figs. 1b and c). Meanwhile the WDM6_EC run failed to produce such a vertically-stacked vortex structure and near-surface winds did not exceed minimum EF-1 intensity (40 ms^{-1}) (Figs. 1e and f).

Graupel which has faster sedimentation velocity than low-density particles mainly hangs over the strong updraft regions. Large amount of graupel is responsible for the localized precipitation over the corresponding region through the accretion process with cloud drops. More snow is generated in the WDM6_EC run with a higher CCN number concentration (cf., Figs. 1c and f), which induces the enhanced horizontal advection of snow with a slower sedimentation velocity relative to graupel. Exaggerated snow-mass loading is responsible for the reduced (increased) rainfall amount over the strong convective core (eyewall) region in the WDM6_EC run.

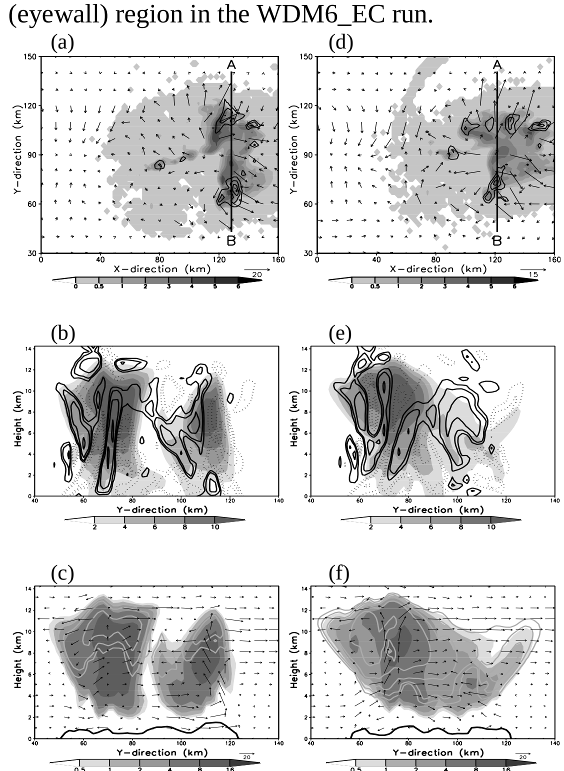

Fig. 1. Low level rain water field (shaded) at 1.75 km, maximum vertical velocity (contour), and storm-relative surface wind vector at 2 hour are represented in (a) and (d). Maximum vertical velocities are contoured at 10 ms^{-1} interval. Vertical cross sections of total mixing ratio (shaded) and vorticity (contour) along the Y-direction are represented in (b) and (e). Contour lines for the vorticity are at ±4, 8, 16, 32×10^{-2} s^{-1} and solid (dotted) lines indicate the positive (negative) value. Cross section for the cold pool defined by the -2℃ isotherm of potential temperature perturbation (thick black line), mixing ratios of graupel (shaded) and snow (thick gray line), and wind vectors are shown in (c) and (f). Contour lines for the snow are at 0.2 0.4 0.8 1.6 3.2 6.4 gkg^{-1}. Cross section regions are denoted in Figure 3a and b as lines 'AB'. Figures on the left panel are for the WDM6_M run and right ones for the WDM6_EC run. Unit for the mixing ratio is gkg^{-1}.

Domain averaged total precipitation with respect to the initial CCN number concentration is shown in Figure 2. When the CCN number concentration is relatively small, the total precipitation is not very sensitive to the CCN number concentration and increases slightly with the CCN number concentration from 100 cm^{-3} to

200 cm^{-3}. The total precipitation decreases sharply when the CCN number concentration is over 200 cm^{-3}, which is the consistent result from Lerach et al. (2008). The reduced precipitation with increasing aerosol is explained by suppressed conversion of cloud droplets to raindrops and reduced convective strength over the strong convective core region with less graupel amount. The precipitation is mainly reduced over the heavy precipitation region near the strong updraft core and slightly increased over the eyewall region of simulated thunder storm (not shown). These characteristics can be also conformed in the storm structure with the WDM6_M and WDM6_EC runs. Time of initial precipitation is delayed in the WDM6_C and WDM6_EC runs (not shown).

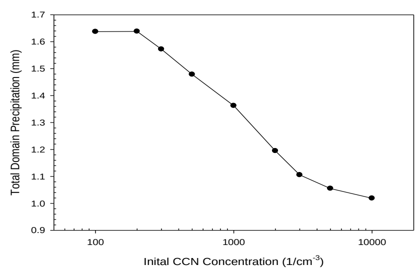

Fig. 2. Total precipitation with respect to the initial CCN number concentration with the WDM6 microphysics scheme.

b. Graupel effects

The importance of graupel substance in simulating convective clouds is stressed from the numerical modeling studies (Zhu and Zhang 2006; Li et al. 2008) and observational one (Houze et al. 1992). To confirm the graupel and graupel-related aerosol effects in simulating convective storm, the WDM5 microphysics scheme was implemented and tested.

Simulated storms show a hook-type structure and move more slowly in the WDM5_M and WDM5_EC runs, compared with the WDM6_M and WDM6_EC runs (Figs. 3a and c). The WDM5 microphysics scheme fails to simulate a right-moving, quasi-steady supercell with two diverging echo masses. The WDM5_M and WDM5_EC runs generate a weaker tornado with the wider cloud coverage along the eyewall. The storm structure does not differ from each other according to the CCN number concentrations with the WDM5 microphysics scheme, however, the intensity of convective core increases with increasing CCN number concentration.

Previous studies mentioned that when there is preexisting rotation at the surface, a downdraft is not needed for tornadogenesis. In these cases, near-ground convergence alone can amplify vertical vorticity to tornado intensity (Wakimoto and Wilson 1989; Roverts and Wilson 1995). Those tornadoes, called as nonsupercell tornadoes, are not occuring with supercell storms, that is, occurring with storms that do not contain mesocyclones. A nonsupercell tornado typically occurs with a storm in its rapid growth stage where the vertical votcity clearly originates near ground and contains a preexisting rotation during its mature stage without flank downdraft. These characteristics are shown in the simulations with the WDM5 microphysics scheme regardless of the CCN number concentration (Figs. 3b and e). Figures 3c and f show the vertical cross section of snow mass and wind fields along the convective core in the WDM5_M and WDM5_EC runs. Without graupel, snow mass loading is abundant across the strong convective core in both experiments, which is responsible for the sporadic rain formation over the eyewall of convective cell region because the accretion process of cloud water by snow is the main source for the precipitation particles in the WDM5 scheme.

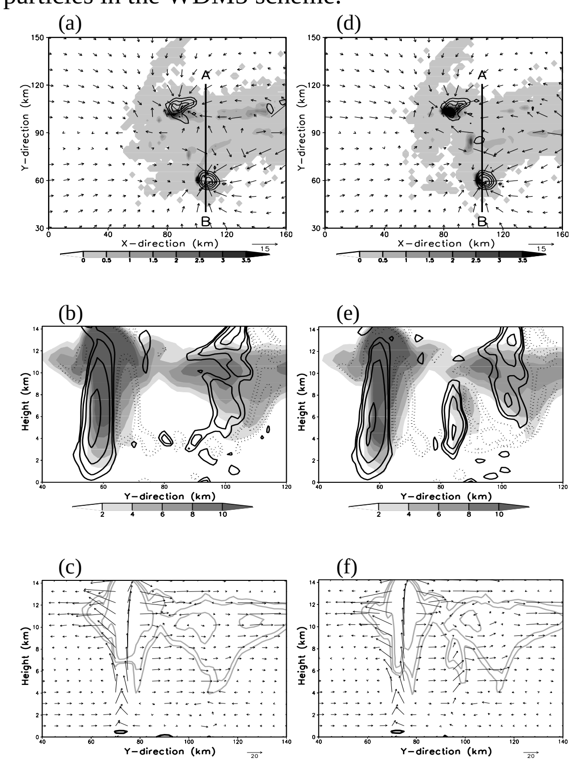

Fig.3. Same as in Figure 3, but with the WDM5_M (left panel) and WDM5_EC (right panel) runs. Contour lines for the snow are at 2, 4, 8, 16, 32, 64 gkg^{-1}.

In terms of the accumulated total precipitation, the experiments with the WDM5 microphysics scheme represent opposite responses under the varying CCN number concentration from the experiments with the WDM6 microphysics scheme (cf., Fig. 2 and 4). The increasing rainfall amount with an increasing CCN number concentration is distinct with the WDM5 microphysics scheme. Figure 5 shows the differences in time-domain averaged mixing ratio of vapor and temperature between the WDM5 (6)_M and WDM5 (6)_EC runs. More saturated environment under the high CCN number concentration with the WDM5 microphysics scheme is responsible for more surface precipitation without further raindrop evaporation. Even though more precipitation reaches to the ground, the effective CCN activation process in the WDM5_EC run results in surface warming. The mixing ratio and temperature profiles with the WDM6 microphysics scheme show different features below the melting level from the WDM5 microphysics. Less saturated environment in the WDM6_EC run causes raindrops to evaporate effectively, compared with the WDM5_EC run. The difference in raindrop diameter between the WDM5_M and WDM5_EC runs is much larger than that between the WDM6_M and WDM6_EC runs. Warming in the upper troposphere in the WDM6_C run indicates the long wave warming with a large mass of the ice phases.

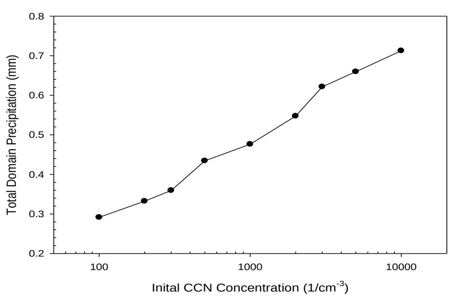

Fig. 4. Same as in Figure 2, but with the WDM5 microphysics scheme

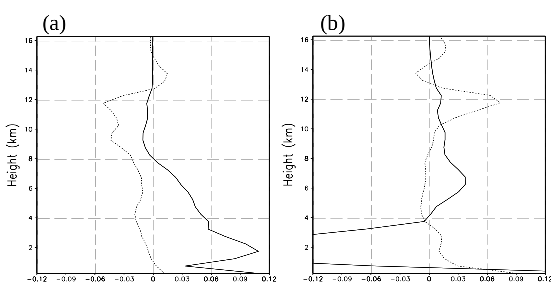

Fig. 5. Vertical profiles of the differences in time-domain averaged mixing ratio of vapor (solid line) and temperature (dotted line). Units for the mixing ratio and temperature are 10 gkg^{-1} and ℃, respectively. Figure 10a and b designate the results for WDM5_EC minus WDM5_M and WDM6_EC minus WDM6_M runs, respectively.

The simulated storm structure in the WDM6_VG experiment is similar with the WDM5_M experiment (not shown). Elongated low-level rain water showing a hook-type structure and convergence of surface wind over the strong convective core is distinct. The WDM6_VG experiment, as in the WDM5_M experiment, fails to simulate a right-moving, quasi-steady supercell, confirming that the denser graupel with relatively strong sedimentation velocity than other ice particles is the essential for maintaining the observed supercell storm structure.

4. Concluding remarks

In the general circulation model (GCM) community, the treatment of aerosol properties and processes is highly simplified and not linked to the precipitation process explicitly in general. Moreover, grid-resolvable precipitation process is considered by diagnostic cloud microphysics schemes (Slingo 1987; Zhao and Carr 1997) or simplified mixed phase microphysics (Dudhia 1989; Grabowski 1998) scheme because of the computational efficiency. However, to understand the aerosol effects properly within the GCM, more sophisticated and refined microphysical processes including the graupel quantity are demandable. Accurate treatment of aerosol should be properly linked to the precipitation process in the GCM. Recently, the double moment scheme, predicting two moments of the size distribution has been developed and implemented into various climate models (e.g., Ghan et al. 1997; Ming et al. 2007; Morrison et al. 2008) and strategies for the accurate representation of aerosol processes have been discussed (Ming et al. 2006; Ghan et al. 2007). With those efforts, a proper evaluation of aerosol effects on the cloud properties and precipitation process could be followed.

Acknowledgements

This work was supported by the project, “Development of the numerical prediction technique for the improved military weather support”, through a grant provided by the Republic of Korea Air Force (ROKAF) in 2009.

References

Lerach, D.G., B. J. Gaudet and W. R. Cotton, 2008: Idealized simulations of aerosol influences on tornadogenesis. *Geophys. Res. Lett.*, **35,** L23806, doi:10.1029/2008GL035617

Weisman, M. L., and J. B. Klemp, 1986: Characteristics of isolated convective storms. *Mesoscale Meteorology and Forecasting*, P. S. Ray, Ed., Amer. Meteor. Soc., 331–358.

Other references will be provided by the author at the request.